

Conformal Prediction via Transported Beta Laws

Thiago R. Ramos

Federal University of São Carlos

THIAGORR@UFSCAR.BR

Helton Graziadei

Federal University of São Carlos

HELTON@UFSCAR.BR

Luben M. C. Cabezas

*Federal University of São Carlos, University of São Paulo,
Inria and Université Grenoble Alpes*

LUCRUZ45.CAB@GMAIL.COM

Abstract

Split conformal prediction provides finite-sample marginal coverage under exchangeability, but this guarantee averages over the random calibration sample. We study instead the law of the calibration-conditional coverage induced by a realized conformal threshold. In the continuous i.i.d. setting this law is exactly $\text{Beta}(k, n + 1 - k)$, so the usual marginal guarantee corresponds to its mean. We take this beta law as a finite-sample reference object and quantify departures from it using Wasserstein distances on $[0, 1]$. The framework yields direct bounds on marginal coverage gaps and on bad-calibration probabilities, and separates different sources of non-i.i.d. behavior according to how they deform the beta reference: test-side shift acts through a transport map on the coverage scale, while calibration dependence changes the order-statistic law itself. We instantiate the framework in scale-shift, clustered, and stationary mixing settings, where the induced deformations can be characterized explicitly or through Berry–Esseen approximations. Simulations on dependent processes confirm that the first-order approximation tracks the empirical Wasserstein distance even at moderate sample sizes.

Keywords: conformal prediction, optimal transport, Wasserstein distance, distribution shift

1. Introduction

Conformal prediction (CP) provides a general framework for constructing prediction sets with finite-sample coverage guarantees (Vovk et al., 2005; Papadopoulos et al., 2002; Lei and Wasserman, 2014). In split conformal prediction, a training sample is used to fit a prediction rule and a separate calibration sample is used to choose a score threshold. For calibration scores S_1, \dots, S_n , with large scores indicating worse conformity, the usual threshold at nominal level $\gamma \in (0, 1)$ is

$$\hat{q}_{n,\gamma} = S_{(k_\gamma)}, \quad k_\gamma = \lceil (n + 1)\gamma \rceil,$$

where $S_{(1)} \leq \dots \leq S_{(n)}$ are the order statistics and $S_{(k)} = +\infty$ for $k > n$. Under exchangeability, this construction satisfies the familiar marginal guarantee

$$\gamma \leq \mathbb{P}(S_{n+1} \leq \hat{q}_{n,\gamma}) < \gamma + \frac{1}{n + 1}.$$

This guarantee is intentionally marginal: the probability averages over the random calibration sample as well as the test score. Once a calibration sample has been drawn, the threshold is fixed; however, across realizations of the calibration sample, the resulting test coverage is itself a random quantity. By the tower property,

$$\mathbb{P}(S_{n+1} \leq \hat{q}_{n,\gamma}) = \mathbb{E}[\mathbb{P}(S_{n+1} \leq \hat{q}_{n,\gamma} | S_1, \dots, S_n)].$$

We call the inner probability the *calibration-conditional coverage*. The usual conformal guarantee controls its mean, but not its sampling distribution.

In the continuous i.i.d. case this distribution has an exact and universal form. For $1 \leq k \leq n$, define

$$C_{n,k} := \mathbb{P}(S_{n+1} \leq S_{(k)} | S_1, \dots, S_n).$$

Then

$$C_{n,k} \sim \text{Beta}(k, n + 1 - k).$$

The beta law is therefore not only a route to the standard marginal coverage bound; it is the finite-sample law of the realized coverage itself (Vovk, 2012; Angelopoulos and Bates, 2021). In a single deployment, the practitioner draws one calibration sample, computes one threshold, and then uses that threshold for future predictions. The realized coverage is one draw from this beta law, while marginal validity constrains only its expectation. For example, with $n = 30$ and $\gamma = 0.9$, so that $k_\gamma = 28$, the reference law is $\text{Beta}(28, 3)$; its lower tail assigns probability about 0.15 to realized coverage below 0.85, and about 0.04 to realized coverage below 0.80. These bad-calibration probabilities are invisible to a statement that only controls the mean.

Figure 1 visualizes this lower-tail effect and its decay with the calibration size.

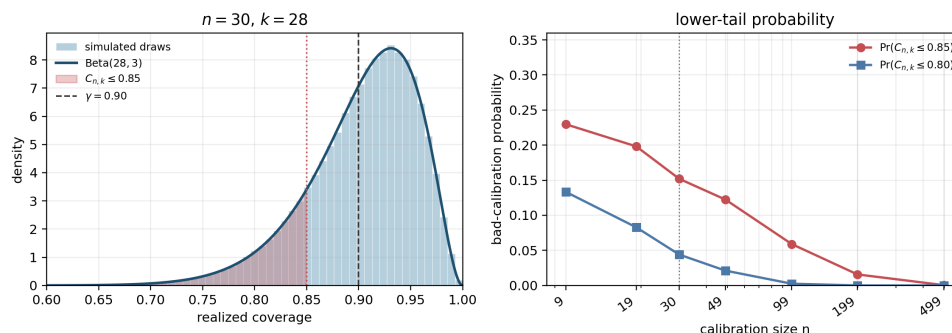


Figure 1: Bad-calibration events under i.i.d. beta reference. Left: simulated draws of $C_{n,k} \sim \text{Beta}(28, 3)$ for $n = 30$, $\gamma = 0.9$, and $k = 28$, with the lower tail $C_{n,k} \leq 0.85$ shaded. Right: simulated lower-tail probabilities for $k = \lceil (n + 1)\gamma \rceil$ as the calibration size increases.

This observation suggests a different way to study conformal prediction beyond the i.i.d. benchmark. Under distribution shift, dependence, or non-identical score distributions, the calibration-conditional coverage need not follow the beta law. Nevertheless, it plays the

same structural role: marginal coverage is obtained by averaging this realized coverage. The central question is therefore how the law of the realized coverage departs from the beta reference, and how that departure translates into coverage degradation.

We address this question using optimal transport on the coverage scale. Rather than transporting calibration and test score distributions directly, we compare the law of the calibration-conditional coverage variable with the beta benchmark on $[0, 1]$. Since the identity map on $[0, 1]$ is 1-Lipschitz, a W_1 comparison on this scale immediately controls the marginal coverage gap. In this sense, the beta law remains the reference object, and non-i.i.d. mechanisms are understood through the way they transport or deform it.

Our contributions are as follows. First, we formulate conformal validity through the law $\nu_{n,k}$ of the realized calibration-conditional coverage and introduce Wasserstein beta neighborhoods around the i.i.d. benchmark $\beta_{n,k} := \text{Beta}(k, n + 1 - k)$. Second, we prove that $W_1(\nu_{n,k}, \beta_{n,k})$ directly bounds the marginal coverage gap and derive corresponding bounds for bad-calibration probabilities. Third, we show how different departures from the i.i.d. benchmark act on the beta reference: test-side shift transports the law on the coverage scale, while calibration dependence changes the order-statistic law itself. Counting-process and Berry–Esseen arguments then provide concrete ways to quantify these deformations. The examples are used to illustrate this framework rather than to define separate procedures.

1.1. Related work

The beta law in conformal prediction. Under continuous i.i.d. scores, the calibration-conditional coverage of split conformal prediction follows a beta distribution (Vovk, 2012; Angelopoulos and Bates, 2021). The i.i.d. assumption can be relaxed to exchangeability. Marques F. (2025) show that, for a test sample exchangeable with the calibration scores, the coverage indicators $Z_i = \mathbf{1}\{S_{n+i} \leq S_{(k)}\}$ form an exchangeable sequence; by de Finetti’s theorem, the empirical coverage converges almost surely as the test sample size grows to a random limit, which a combinatorial argument identifies as a beta law. We work in the i.i.d. framing for notational simplicity and because it gives the probability integral transform used in our Wasserstein analysis.

Conformal prediction and optimal transport. A growing line of work applies optimal transport tools to conformal prediction under distribution shift, but the transported object differs from ours. Xu et al. (2025) bound the coverage gap under joint covariate and concept shift using the 1-Wasserstein distance between calibration and test score distributions, and use the bound as a training regularizer. Correia and Louizos (2025) derive coverage-gap bounds formulated via optimal transport distances on the score space and use unlabeled test data to attenuate the gap. Aolaritei et al. (2025) model distribution shift through Levy–Prokhorov ambiguity sets propagated through the score function, reducing a high-dimensional shift to a one-dimensional problem on the score scale. These approaches compare score laws, transported weights, or ambiguity sets. Our comparison takes place after calibration: the transported object is the law of the realized coverage itself on $[0, 1]$. This is what makes the Kantorovich–Rubinstein duality immediately yield a marginal coverage-gap bound, without an intermediate quantile-level argument.

Conformal prediction beyond exchangeability. Several other lines of work quantify how violations of exchangeability affect split conformal coverage. Barber et al. (2023)

develop non-exchangeable conformal prediction via weighted quantiles and nonsymmetric algorithms, with finite-sample bounds that degrade in the total variation distance to a reference exchangeable law. Oliveira et al. (2024) show that vanilla split conformal prediction remains valid for a broad class of non-exchangeable processes, including time series and spatiotemporal data, at the cost of a small coverage penalty controlled by concentration and decoupling arguments. In contrast, we replace total-variation or mixing-type penalties on the data-generating law with W_1 distances between realized-coverage laws.

A related asymptotic literature studies the joint behavior of conformal coverage across a test sample. Gazin et al. (2024) show that the joint distribution of conformal p -values in a full conformal setting is a Pólya urn and prove a concentration inequality for their empirical c.d.f. under exchangeability. Gazin (2024) identify the asymptotic distribution of the false coverage proportion as $n, m \rightarrow \infty$, recovering the Kolmogorov law after rescaling, with extensions to weighted conformal and covariate shift. By contrast, our object is finite-sample and fixed-quantile: the law of $(C_{n,k})$, together with its non-i.i.d. analogue. The Pólya urn and Brownian bridge representations offer complementary large-test-sample descriptions; here we instead study how the finite-sample beta law itself is transported under shift and dependence.

2. Background

This section develops the theoretical background required for the remainder of the paper.

2.1. Conformal prediction

We recall the basic split conformal construction and the two classical facts that will serve as reference points throughout the paper. The first is the usual finite-sample marginal coverage guarantee. The second is a more refined description of the random coverage level induced by the realized calibration sample.

Let $S \sim F_S$ be a continuous score distribution, and let S_1, \dots, S_n denote calibration scores on this scale. In the i.i.d. case, these scores form an independent sample from F_S . Define the *adjusted empirical conformal γ -quantile* as

$$\hat{q}_{n,\gamma} = S_{(\lceil \gamma(n+1) \rceil)},$$

with the convention that $S_{(k)} = +\infty$ whenever $k > n$.¹

The conformal threshold is therefore an empirical order statistic of the calibration scores. The use of $\lceil \gamma(n+1) \rceil$ rather than the usual empirical quantile index is the finite-sample correction that makes the split conformal guarantee hold without asymptotics.

Theorem 1 (Split Conformal Marginal Coverage) *Assume that S_1, \dots, S_n, S_{n+1} are exchangeable and that there are no ties almost surely. Let $k_\gamma = \lceil (n+1)\gamma \rceil$ and $\hat{q}_{n,\gamma} = S_{(k_\gamma)}$, with the convention that $S_{(k)} = +\infty$ whenever $k > n$. Then*

$$\gamma \leq \mathbb{P}(S_{n+1} \leq \hat{q}_{n,\gamma}) < \gamma + \frac{1}{n+1}.$$

1. This definition—using $n+1$ in place of n —is standard in conformal prediction, as it guarantees finite-sample marginal coverage of at least γ : $\mathbb{P}(S_{n+1} \leq \hat{q}_{n,\gamma}) \geq \gamma$.

The proof of this statement is elementary and relies on the uniformity of ranks. This is the classical finite-sample marginal coverage guarantee of split conformal prediction. It is the benchmark statement: under exchangeability, the conformal threshold covers a fresh score with probability at least γ , up to the unavoidable discretization error of order $(n+1)^{-1}$.

For our purposes, however, the marginal guarantee is only the first layer of the story. Once the calibration sample is realized, the order statistic $S_{(k)}$ is fixed, and the coverage of this realized threshold is itself a random quantity as the calibration sample varies. We next describe the distribution of this calibration-conditional coverage for a fixed order statistic.

Proposition 2 *Let $S \sim F_S$ be a continuous random variable and let $\{S_i\}_{i=1}^n$ be an i.i.d. sample from F_S . For $1 \leq k \leq n$, define*

$$C_{n,k} = \mathbb{P}(S_{n+1} \leq S_{(k)} \mid S_1, \dots, S_n).$$

Then

$$C_{n,k} = F_S(S_{(k)}) \sim \text{Beta}(k, n+1-k).$$

The proof is given in Appendix A.1. This proposition gives a conditional refinement of the marginal CP guarantee. It says that, in the continuous i.i.d. setting, the realized coverage of the threshold $S_{(k)}$ is not arbitrary: its law is exactly the beta law associated with the corresponding order statistic.

Throughout the paper, we write

$$\beta_{n,k} := \text{Beta}(k, n+1-k)$$

for this i.i.d. reference law.

In particular, letting $k_\gamma = \lceil (n+1)\gamma \rceil$, Proposition 2 gives us

$$\begin{aligned} \mathbb{P}(S_{n+1} \leq \hat{q}_{n,\gamma}) &= \mathbb{E}[\mathbb{P}(S_{n+1} \leq \hat{q}_{n,\gamma} \mid S_1, \dots, S_n)] \\ &= \mathbb{E}[C_{n,k_\gamma}] \\ &= \frac{\lceil (n+1)\gamma \rceil}{n+1} \in \left[\gamma, \gamma + \frac{1}{n+1} \right], \end{aligned}$$

which recovers the classic CP upper and lower bounds.

The same beta law also gives a precise way to discuss bad calibration. A bad calibration event occurs when the realized coverage produced by the calibration sample is substantially below the nominal level. The marginal split conformal guarantee controls only the mean of $C_{n,k}$; the lower tail of the beta law controls how often an unfavorable calibration sample occurs.

Theorem 3 (i.i.d. Bad Calibration Probabilities) *Under the assumptions of Proposition 2, let $B_{n,k} \sim \beta_{n,k}$. Then, for every $t \in [0, 1]$,*

$$\mathbb{P}(C_{n,k} \leq t) = \mathbb{P}(B_{n,k} \leq t).$$

In particular, if $k_\gamma = \lceil (n+1)\gamma \rceil \leq n$, then, for every $\eta \in (0, \gamma)$,

$$\mathbb{P}(C_{n,k_\gamma} \leq \gamma - \eta) = \mathbb{P}(B_{n,k_\gamma} \leq \gamma - \eta).$$

This follows immediately from Proposition 2. It identifies the beta lower tail as the i.i.d. reference probability of a bad calibration event. Later, when the realized coverage law is no longer exactly beta, our Wasserstein bounds will compare its lower tail to this same reference quantity.

Thus, the classical split conformal guarantee is recovered as the mean of this beta law. The rest of the paper takes this beta distribution as the reference law: departures from the i.i.d. setting will be measured by how much the realized conditional coverage law deviates from this beta benchmark.

2.2. Optimal Transport and Wasserstein Distance

We recall the few facts about Wasserstein distances that will be used below (Ambrosio et al., 2005; Villani, 2009; Peyré and Cuturi, 2019; Santambrogio, 2015). Let (\mathcal{X}, d) be a metric space. For $p \geq 1$, the p -Wasserstein distance between probability laws μ and ν is

$$W_p(\mu, \nu) = \left(\inf_{\pi \in \Pi(\mu, \nu)} \int_{\mathcal{X} \times \mathcal{X}} d(x, y)^p d\pi(x, y) \right)^{1/p},$$

where $\Pi(\mu, \nu)$ is the set of couplings with marginals μ and ν . On the space of probability laws with finite p -th moment, W_p is a metric. In particular, when $\mathcal{X} = [0, 1]$, the moment condition is automatic.

In this paper, the laws compared by Wasserstein distances are laws of calibration-conditional coverage variables, supported on $[0, 1]$. In this setting, with $d(u, v) = |u - v|$, the definition becomes

$$W_p(\mu, \nu) = \left(\inf_{\pi \in \Pi(\mu, \nu)} \int_{[0, 1]^2} |u - v|^p d\pi(u, v) \right)^{1/p}.$$

We first record two elementary consequences of the definition.

Proposition 4 (Coupling Upper Bound) *Fix $p \geq 1$. Let μ and ν be probability laws on $[0, 1]$. If $X \sim \mu$ and $Y \sim \nu$ are defined on the same probability space, then*

$$W_p(\mu, \nu) \leq (\mathbb{E}[|X - Y|^p])^{1/p}.$$

This bound is our basic way of turning a concrete coupling into a Wasserstein estimate. The next fact explains how estimates at different Wasserstein orders are related.

Proposition 5 (Monotonicity in p) *Let μ and ν be probability laws on $[0, 1]$. If $1 \leq p \leq q$, then*

$$W_p(\mu, \nu) \leq W_q(\mu, \nu).$$

This monotonicity lets us state some intermediate estimates in the Wasserstein order that is most convenient and then read them on the W_1 scale used for coverage.

For estimates involving expectations, we will also use the following dual form of W_1 .

Proposition 6 (Dual Representation and Mean Bound) *If μ and ν are probability measures on $[0, 1]$, then*

$$W_1(\mu, \nu) = \sup_{\|f\|_{\text{Lip}} \leq 1} \left| \int f(u) d\mu(u) - \int f(u) d\nu(u) \right|.$$

In particular,

$$\left| \int u d\mu(u) - \int u d\nu(u) \right| \leq W_1(\mu, \nu).$$

The first identity in Proposition 6 is the Kantorovich–Rubinstein duality (Santambrogio, 2015, Eq. (3.1)). The second follows by taking the identity map $u \mapsto u$, which is 1-Lipschitz on $[0, 1]$. Together with Proposition 5, this means that any W_p bound with $p \geq 1$ can be converted into the corresponding mean bound through W_1 when needed.

Proposition 7 (Optimality of Monotone Transport) *Fix $p \geq 1$. Let μ and ν be probability laws on \mathbb{R} with finite p -th moments. Assume that F_μ is continuous, and let F_ν^{-1} denote the generalized inverse of F_ν . Define*

$$T_{\text{mon}}(x) = F_\nu^{-1}(F_\mu(x)).$$

If $X \sim \mu$, then $T_{\text{mon}}(X) \sim \nu$, and the coupling $(X, T_{\text{mon}}(X))$ is optimal. Consequently,

$$W_p^p(\mu, \nu) = \mathbb{E}[|X - T_{\text{mon}}(X)|^p].$$

This is the one-dimensional monotone rearrangement theorem (Santambrogio, 2015, Thm. 2.9). It gives an explicit optimal map, which will be useful when a distorted realized-coverage law can be transported back to its beta reference.

Proposition 8 (One-Dimensional Formula) *Let μ and ν be probability laws on $[0, 1]$, with distribution functions F_μ and F_ν . Then*

$$W_1(\mu, \nu) = \int_0^1 |F_\mu(t) - F_\nu(t)| dt.$$

Proposition 8 will be useful when the calibration-conditional coverage law is described through an order statistic or through the associated counting process.

Although our main objects are supported on $[0, 1]$, some asymptotic calculations below compare Gaussian limits on \mathbb{R} . We will use the following closed form for centered normal laws, where W_1 is computed with the Euclidean distance.

Lemma 9 (Centered Normal Laws) *For any $\sigma_1, \sigma_2 \geq 0$,*

$$W_1(N(0, \sigma_1^2), N(0, \sigma_2^2)) = \sqrt{\frac{2}{\pi}} |\sigma_1 - \sigma_2|.$$

3. A Transportation Framework for Conformal Prediction

In the previous section, we identified $\beta_{n,k}$ as the law of the realized coverage induced by the k -th conformal order statistic in the continuous i.i.d. setting. We now use this beta law as a reference object. A calibration and test mechanism induces a law for its realized coverage, and the main question is how much this law differs from the i.i.d. beta benchmark.

Fix $1 \leq k \leq n$, and let

$$\mathcal{C}_n = (T_1, \dots, T_n)$$

be the calibration scores under a joint law P . Let \tilde{T} denote the test score.² This notation does not tie the test score to the next index after calibration; for example, in a time-series setting one may take $\tilde{T} = T_{n+h}$, with h fixed or depending on n . Let the calibration order statistics be

$$T_{(1)} \leq \dots \leq T_{(n)}.$$

The marginal coverage of the threshold $T_{(k)}$ is

$$\text{Cov}(k) := \mathbb{P}(\tilde{T} \leq T_{(k)}).$$

We write it as the expectation of the coverage realized by the particular calibration sample:

$$D_{n,k} := \mathbb{P}(\tilde{T} \leq T_{(k)} \mid \mathcal{C}_n).$$

Thus

$$\text{Cov}(k) = \mathbb{E}[D_{n,k}].$$

The law of this random realized coverage is

$$\nu_{n,k} := \mathcal{L}(D_{n,k}).$$

In the continuous i.i.d. reference case, Proposition 2 gives $\nu_{n,k} = \beta_{n,k}$. The framework below keeps $\beta_{n,k}$ fixed as the benchmark and measures the deformation from $\beta_{n,k}$ to $\nu_{n,k}$ on the coverage scale $[0, 1]$. This leads to the following convenient notation.

Definition 10 (Wasserstein Beta Neighborhood) *Let $\mathcal{P}([0, 1])$ denote the set of probability laws on $[0, 1]$. For $p \geq 1$ and $\rho \geq 0$, define*

$$\mathcal{B}_p(\beta_{n,k}, \rho) := \{\nu \in \mathcal{P}([0, 1]) : W_p(\nu, \beta_{n,k}) \leq \rho\}.$$

We say that the realized coverage law is in the p -Wasserstein beta neighborhood of radius ρ when

$$\nu_{n,k} \in \mathcal{B}_p(\beta_{n,k}, \rho).$$

The radius ρ quantifies how far the realized coverage law is from the i.i.d. beta law. When $\rho = 0$, the realized coverage law is exactly the beta reference; for positive ρ , it is a transported or perturbed version of that reference. To make this geometric picture concrete, consider the contaminated law $\nu_{\pi,c} = (1 - \pi)\beta_{n,k} + \pi\delta_c$, which replaces a fraction π of the

2. Throughout the text, S_i denotes i.i.d. scores, while T_i denotes scores that need not be i.i.d.

beta mass by a point mass at coverage value $c \in [0, 1]$. A direct computation via Proposition 8 gives

$$W_1(\nu_{\pi,c}, \beta_{n,k}) = \pi \int_0^1 |\mathbf{1}\{x \geq c\} - F_\beta(x)| dx,$$

so the radius grows linearly in π at a rate determined by how far c sits from the bulk of $\beta_{n,k}$. Figure 2 displays this as a function of (π, c) , with each contour tracing the boundary of the Wasserstein ball $\mathcal{B}_1(\beta_{n,k}, \rho)$ for a different radius ρ . The shape of these contours reflects the geometry of the contamination: for c close to γ , the point mass lands near the bulk of $\beta_{n,k}$ and transport is cheap, so the contour allows a larger contamination fraction π before the radius ρ is exceeded. As c moves away from γ , the transport cost per unit of π increases, and the contour bends inward, permitting only a smaller π for the same budget ρ . Each contour therefore defines a feasible region in (π, c) : staying inside it is precisely the condition $\nu_{\pi,c} \in \mathcal{B}_1(\beta_{n,k}, \rho)$.

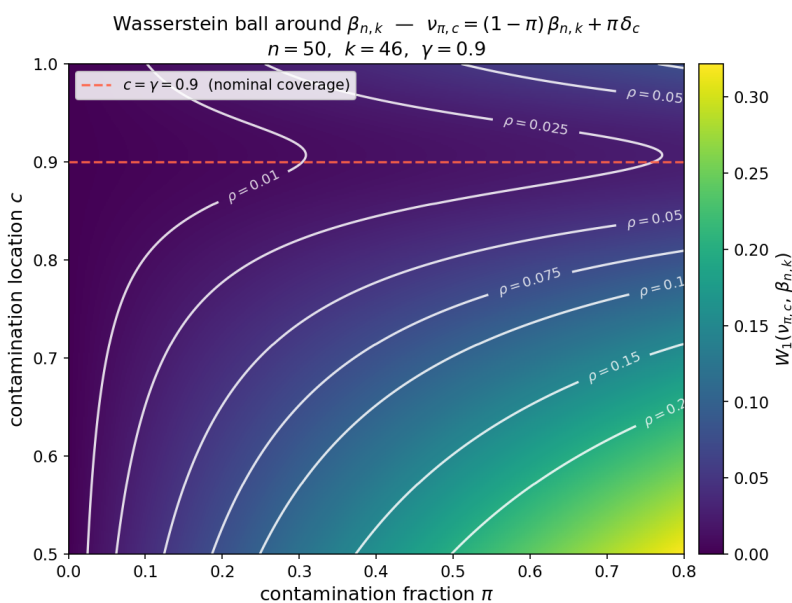


Figure 2: Wasserstein radius $W_1(\nu_{\pi,c}, \beta_{n,k})$ for the contaminated law $\nu_{\pi,c} = (1-\pi)\beta_{n,k} + \pi\delta_c$, with $n = 50$, $k = 46$, and $\gamma = 0.9$. Each white contour traces the boundary of $\mathcal{B}_1(\beta_{n,k}, \rho)$ for a given ρ , defining the set of contaminations (π, c) compatible with that transport budget. Contamination near $c = \gamma$ allows a larger fraction π for the same radius, while contamination away from γ forces π to be small — the contour shape directly encodes this trade-off.

3.1. Coverage Guarantees

The first consequence of a Wasserstein comparison is a direct bound on marginal coverage. This is the basic reason for working on the coverage scale.

Theorem 11 (Wasserstein Coverage Gap) Fix $1 \leq k \leq n$, and define $D_{n,k}$, $\nu_{n,k}$, and $\text{Cov}(k)$ as above. Then

$$\left| \text{Cov}(k) - \frac{k}{n+1} \right| \leq W_1(\nu_{n,k}, \beta_{n,k}).$$

Consequently, if $\nu_{n,k} \in \mathcal{B}_p(\beta_{n,k}, \rho)$ for some $p \geq 1$, then

$$\left| \text{Cov}(k) - \frac{k}{n+1} \right| \leq \rho.$$

If $k_\gamma = \lceil (n+1)\gamma \rceil \leq n$, then

$$|\text{Cov}(k_\gamma) - \gamma| \leq \rho + \frac{1}{n+1}.$$

The proof is given in Appendix A.2. The theorem says that once the realized coverage law is close to the beta benchmark in Wasserstein distance, the usual conformal coverage level degrades by at most the same amount, up to the standard discretization term.

The previous result controls the average of $D_{n,k}$. We can also ask for the probability that a realized calibration sample produces unusually low coverage. A Wasserstein beta neighborhood gives a comparison with the lower tail of the beta reference.

Theorem 12 (Bad Calibration Probabilities) Let $B_{n,k} \sim \beta_{n,k}$. If

$$\nu_{n,k} \in \mathcal{B}_p(\beta_{n,k}, \rho)$$

for some $p \geq 1$, then, for every $t \in [0, 1]$ and every $\varepsilon > 0$,

$$\mathbb{P}(D_{n,k} \leq t) \leq \mathbb{P}(B_{n,k} \leq t + \varepsilon) + \left(\frac{\rho}{\varepsilon}\right)^p.$$

The proof is given in Appendix A.3. The beta term is the probability of a bad calibration event in the i.i.d. reference model; the additional term accounts for the transport needed to move the beta law to the realized coverage law. The Markov penalty is useful when only an average transport radius is available, but it can be conservative, especially on the W_1 scale.

When the deformation from the beta law can be bounded uniformly, the bad calibration comparison takes a sharper form. Let

$$T_{\text{mon}} = F_{\nu_{n,k}}^{-1} \circ F_{\beta_{n,k}}$$

be the monotone transport map from $\beta_{n,k}$ to $\nu_{n,k}$, and let $B_{n,k} \sim \beta_{n,k}$. If

$$|T_{\text{mon}}(B_{n,k}) - B_{n,k}| \leq \rho \quad \text{a.s.},$$

then for every $t \in [0, 1]$,

$$\mathbb{P}(D_{n,k} \leq t) \leq \mathbb{P}(B_{n,k} \leq t + \rho).$$

Indeed, under this coupling $D_{n,k} \stackrel{d}{=} T_{\text{mon}}(B_{n,k})$, and $T_{\text{mon}}(B_{n,k}) \leq t$ implies $B_{n,k} \leq t + \rho$.

Thus a uniform transport bound shifts the beta lower tail without the Markov penalty appearing in Theorem 12. This is the cleanest version of the transported-beta picture, and we use it whenever an explicit transport map is available.

3.2. Decoupled Test Scores and Transported Beta Laws

A particularly useful simplification occurs when the test score is decoupled from the calibration sample. This assumption is natural in independent holdout evaluation and in distribution-shift settings with separate calibration and test batches. It is also a useful reduction for temporally dependent data when the test point is sufficiently separated from the calibration block and the dependence decays with the lag.

Proposition 13 (Decoupled Test Scores) *Assume that \tilde{T} is independent of \mathcal{C}_n , and let $F_{\tilde{T}}$ be its distribution function. Then*

$$D_{n,k} = F_{\tilde{T}}(T_{(k)}), \quad \nu_{n,k} = \mathcal{L}(F_{\tilde{T}}(T_{(k)})).$$

Suppose that the calibration scores have a common continuous marginal distribution function F_T , and let F_T^{-1} denote its generalized inverse. Define

$$U_i := F_T(T_i), \quad i = 1, \dots, n.$$

Then the variables U_i are marginally uniform on $[0, 1]$, possibly dependent, and, for $h := F_{\tilde{T}} \circ F_T^{-1}$, we have

$$D_{n,k} \stackrel{d}{=} h(U_{(k)}), \quad \nu_{n,k} = h_{\#}\mathcal{L}(U_{(k)}).$$

The proof is given in Appendix A.4. In the no-shift case $F_{\tilde{T}} = F_T$, the map h is the identity and $\nu_{n,k} = \mathcal{L}(U_{(k)})$, so Theorem 11 reduces coverage analysis to

$$W_1(\mathcal{L}(U_{(k)}), \beta_{n,k}).$$

The following proposition records the counting-process representation of this distance.

Proposition 14 (Counting Formula) *Let U_1, \dots, U_n be random variables on $[0, 1]$. Assume each U_i is uniform; independence is not required. Let*

$$F_n(t) := \frac{1}{n} \sum_{i=1}^n \mathbf{1}\{U_i \leq t\}, \quad N_n(t) := nF_n(t).$$

Then, for every $t \in [0, 1]$ and $1 \leq k \leq n$,

$$\{U_{(k)} \leq t\} = \{N_n(t) \geq k\}.$$

Consequently, if $Z_{n,t} \sim \text{Bin}(n, t)$, then

$$W_1(\mathcal{L}(U_{(k)}), \beta_{n,k}) = \int_0^1 |\mathbb{P}(N_n(t) \geq k) - \mathbb{P}(Z_{n,t} \geq k)| dt.$$

The proof is given in Appendix A.5. Thus the Wasserstein distance to the beta law is exactly the integrated difference between the dependent empirical-count tail and the binomial tail.

3.3. Berry–Esseen Transport for Dependent Calibration

In many dependent calibration settings, the law of $U_{(k)}$ is not exactly beta, but it admits a Berry–Esseen approximation. This is enough to control its Wasserstein distance to the beta reference.

Let U_1, \dots, U_n be marginally uniform random variables on $[0, 1]$, not necessarily independent, and fix $\gamma \in (0, 1)$. Here Φ denotes the standard normal distribution function. Suppose that, for some $\tau_\gamma > 0$ and some deterministic sequence $a_n \rightarrow 0$,

$$\sup_{x \in \mathbb{R}} \left| \mathbb{P}(\sqrt{n}\{U_{(k_\gamma)} - \gamma\} \leq x) - \Phi\left(\frac{x}{\tau_\gamma}\right) \right| \leq a_n.$$

This assumption says that the calibration order statistic has a Berry–Esseen law with asymptotic standard deviation τ_γ . The i.i.d. beta reference has the same form with standard deviation $\sqrt{\gamma(1-\gamma)}$.

Proposition 15 (Quantile-to-Beta Transport) *If the preceding Berry–Esseen bound holds, then*

$$W_1(\mathcal{L}(U_{(k_\gamma)}), \beta_{n, k_\gamma}) \leq a_n + \sqrt{\frac{2}{\pi n}} \left| \tau_\gamma - \sqrt{\gamma(1-\gamma)} \right| + O(n^{-1/2}).$$

In particular, if $a_n = O(n^{-1/2})$, then

$$W_1(\mathcal{L}(U_{(k_\gamma)}), \beta_{n, k_\gamma}) \leq \sqrt{\frac{2}{\pi n}} \left| \tau_\gamma - \sqrt{\gamma(1-\gamma)} \right| + O(n^{-1/2}).$$

The proof is given in Appendix [A.7](#).

In the next section, we apply this framework in several concrete settings. The examples differ in how the beta law is deformed, but the logic is the same: identify the realized coverage law, compare it with $\beta_{n, k}$, and translate that comparison into a coverage statement.

4. Applications

4.1. Exact Transported Beta Laws under Distribution Shift

We first consider a decoupled distribution-shift setting. The calibration scores are i.i.d. from a continuous distribution function F_T , while the test score is independent of the calibration sample but follows a possibly different distribution function $F_{\tilde{T}}$. Let F_T^{-1} denote the generalized inverse, or quantile function, of the calibration score distribution. The conformal threshold $T_{(k)}$ is therefore generated under the calibration law, but its coverage is evaluated under the test law.

For a realized calibration sample, the realized test coverage is

$$D_{n, k} := \mathbb{P}\left(\tilde{T} \leq T_{(k)} \mid T_1, \dots, T_n\right) = F_{\tilde{T}}(T_{(k)}).$$

Since the calibration sample is i.i.d. with distribution function F_T , the probability integral transform gives

$$B_{n, k} := F_T(T_{(k)}) \sim \beta_{n, k}.$$

Thus the shifted realized coverage can be written on the beta scale as

$$D_{n,k} = F_{\tilde{T}}(F_T^{-1}(B_{n,k})).$$

Equivalently, if $h := F_{\tilde{T}} \circ F_T^{-1}$, then

$$D_{n,k} \stackrel{d}{=} h(B_{n,k}), \quad \nu_{n,k} = h_{\#}\beta_{n,k}.$$

Distribution shift therefore does not alter the beta order-statistic mechanism itself. It transports the beta law through the map relating calibration and test score distributions. When $F_{\tilde{T}} = F_T$, the map h is the identity and $\nu_{n,k} = \beta_{n,k}$, recovering the i.i.d. reference case. In general, the relevant comparison is

$$W_1(\nu_{n,k}, \beta_{n,k}) = W_1((F_{\tilde{T}} \circ F_T^{-1})_{\#}\beta_{n,k}, \beta_{n,k}).$$

We illustrate the distribution-shift mechanism in a setting where the transport map is explicit.

4.1.1. EXAMPLE: HALF-NORMAL SCALE SHIFT

The example is motivated by the usual split conformal regression score

$$T = |Y - \hat{\mu}(X)|.$$

If the prediction error is centered Gaussian, then T has a half-normal distribution. Let

$$T_1, \dots, T_n \stackrel{\text{iid}}{\sim} |N(0, \sigma_T^2)|, \quad \tilde{T} \sim |N(0, \sigma_{\tilde{T}}^2)|,$$

with \tilde{T} independent of the calibration sample, and define the scale ratio

$$r := \frac{\sigma_{\tilde{T}}}{\sigma_T}.$$

Writing $q(u) := \Phi^{-1}\left(\frac{u+1}{2}\right)$, the calibration-to-test transport map is

$$h_r(u) = 2\Phi\left(\frac{q(u)}{r}\right) - 1.$$

Thus, if $B_{n,k} := F_{\sigma_T}(T_{(k)}) \sim \beta_{n,k}$, then the realized coverage under the shifted test distribution satisfies

$$D_{n,k} = F_{\sigma_{\tilde{T}}}(T_{(k)}) \stackrel{d}{=} h_r(B_{n,k}), \quad \nu_{n,k}^{(r)} = (h_r)_{\#}\beta_{n,k}.$$

Therefore, in the half-normal scale-shift model, distribution shift does not alter the beta order-statistic law on the calibration scale; it transports this law through the deterministic map h_r . Details on the derivation of h_r , its inverse, and the corresponding density transformation are given in Appendix A.6.

The direction of the deformation is determined by r . If $r > 1$, the test scores are more dispersed than the calibration scores and $h_r(u) < u$, leading to undercoverage. If $r < 1$, then $h_r(u) > u$, leading to overcoverage. Moreover,

$$\text{Cov}(k) = \mathbb{E}[h_r(B_{n,k})],$$

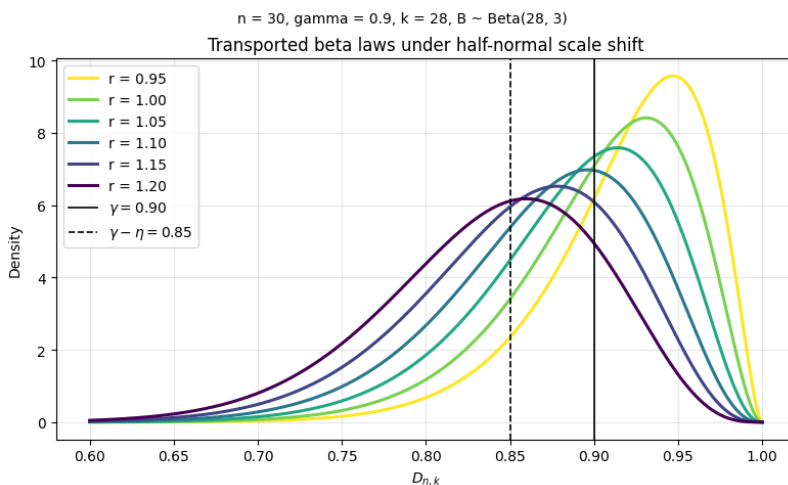


Figure 3: Transported beta laws under half-normal scale shift for $n = 30$, $\gamma = 0.9$, and $k = 28$, so that $B_{n,k} \sim \text{Beta}(28, 3)$. Under the scale ratio $r = \sigma_{\tilde{T}}/\sigma_T$, the realized coverage satisfies $D_{n,k} \stackrel{d}{=} h_r(B_{n,k})$. As r increases above one, the law is transported to the left, increasing the probability of bad calibration. The vertical lines mark $\gamma = 0.90$ and $\gamma - \eta = 0.85$, with $\eta = 0.05$.

so that

$$\text{Cov}(k) - \frac{k}{n+1} = \mathbb{E}[h_r(B_{n,k}) - B_{n,k}].$$

In this example, the Wasserstein coverage-gap bound is:

$$W_1(\nu_{n,k}^{(r)}, \beta_{n,k}) = \left| \text{Cov}(k) - \frac{k}{n+1} \right|.$$

Figure 3 illustrates the induced deformation for $n = 30$, $\gamma = 0.9$, and $k = \lceil (n+1)\gamma \rceil = 28$, so that the i.i.d. reference law is $\text{Beta}(28, 3)$. The curve $r = 1$ corresponds to this reference law. As r increases above one, the realized-coverage law is transported to the left, increasing the probability of low calibration-conditional coverage. The vertical lines mark the nominal level $\gamma = 0.9$ and the bad-calibration threshold $\gamma - \eta = 0.85$, with $\eta = 0.05$.

For small scale shifts, writing $r = e^\delta$, the local approximation derived in Appendix A.6 gives

$$\text{Cov}(k_\gamma) - \gamma = -2\delta \phi(q(\gamma))q(\gamma) + O(\delta^2) + O(n^{-1}), \quad q(\gamma) = \Phi^{-1}\left(\frac{\gamma+1}{2}\right).$$

At $\gamma = 0.9$, the coefficient $2\phi(q(\gamma))q(\gamma)$ is approximately 0.339. Thus a 10% increase in the test-score scale, $r = 1.1$, corresponds to an approximate coverage loss of about 0.032, or roughly three percentage points.

Thus, in the half-normal scale-shift model, the abstract Wasserstein coverage-gap bound becomes an exact identity: the transport distance from the beta reference is precisely the

marginal coverage loss, and the transported law determines bad-calibration probabilities through its left tail $\mathbb{P}(h_r(B_{n,k}) \leq t)$. Figure 5 in Appendix A.6 makes this concrete across $r \in \{0.5, 0.8, 2.0\}$ and $n \in \{50, 200, 1000\}$: the shaded area between the CDFs grows with $|r - 1|$ and is insensitive to n , while the right panel reveals that W_1 is asymmetric around $r = 1$, with undercoverage ($r > 1$) incurring a larger transport cost than overcoverage ($r < 1$) for the same departure, reflecting the nonlinearity of h_r and the concentration of $\beta_{n,k}$ near γ .

4.2. Clustered Calibration and Effective Sample Size

Proposition 14 has a simple concrete instance in clustered or replicated calibration data. Think of b independent experimental units, subjects, videos, or spatial locations, each producing m nearly identical calibration scores, so that $n = mb$. The following idealized model takes the within-cluster dependence to be perfect. Let

$$V_1, \dots, V_b \stackrel{\text{iid}}{\sim} \text{Unif}(0, 1),$$

and set

$$U_{j,r} = V_j, \quad j = 1, \dots, b, \quad r = 1, \dots, m,$$

and then relabel $\{U_{j,r}\}$ as U_1, \dots, U_n . Each U_i is still marginally uniform, but the effective number of independent calibration units is b , not n . Indeed,

$$N_n(t) = \sum_{i=1}^n \mathbf{1}\{U_i \leq t\} = m \sum_{j=1}^b \mathbf{1}\{V_j \leq t\},$$

so $N_n(t) \stackrel{d}{=} mZ_{b,t}$, with $Z_{b,t} \sim \text{Bin}(b, t)$. Proposition 14 gives

$$W_1(\mathcal{L}(U_{(k)}), \beta_{n,k}) = \int_0^1 |\mathbb{P}(Z_{b,t} \geq \lceil k/m \rceil) - \mathbb{P}(Z_{n,t} \geq k)| dt, \quad Z_{n,t} \sim \text{Bin}(n, t).$$

Equivalently,

$$U_{(k)} = V_{(\lceil k/m \rceil)} \quad \text{a.s.},$$

and therefore

$$U_{(k)} \sim \text{Beta}(\lceil k/m \rceil, b + 1 - \lceil k/m \rceil).$$

This example is an extreme cluster model and creates ties within the calibration block. The counting identity and the Wasserstein comparison do not require absence of ties, but the example can also be viewed as the limit of a model with small within-cluster jitter. Its purpose is to isolate the practical effect: using n highly clustered calibration points behaves, for the realized coverage law, more like using b independent calibration units.

Thus, in the no-shift decoupled-test version of this application, $D_{n,k} \stackrel{d}{=} U_{(k)}$. If

$$\rho_{\text{cl}}(k) := W_1(\text{Beta}(\lceil k/m \rceil, b + 1 - \lceil k/m \rceil), \beta_{n,k}),$$

then Theorem 11 gives

$$\left| \text{Cov}(k) - \frac{k}{n+1} \right| \leq \rho_{\text{cl}}(k).$$

For $k_\gamma = \lceil (n+1)\gamma \rceil$, the target level is therefore degraded by at most $\rho_{\text{cl}}(k_\gamma) + 1/(n+1)$. Theorem 12 also gives, for every $t \in [0, 1]$ and $\varepsilon > 0$,

$$\mathbb{P}(D_{n,k} \leq t) \leq \mathbb{P}(B_{n,k} \leq t + \varepsilon) + \frac{\rho_{\text{cl}}(k)}{\varepsilon}, \quad B_{n,k} \sim \beta_{n,k}.$$

In this example, both conclusions say that clustering affects conformal coverage only through the transport from the nominal beta law based on n points to the effective beta law based on b independent units.

4.3. Stationary Mixing Processes

We now apply Proposition 15 to a stationary score process $(T_i)_{i \in \mathbb{Z}}$. Let F_T be its continuous marginal distribution function. The calibration sample is $\mathcal{C}_n = (T_1, \dots, T_n)$, and the test score is taken ℓ steps after the calibration block:

$$\tilde{T} = T_{n+\ell}, \quad \ell \geq 1.$$

The transformed variables $U_i = F_T(T_i)$ are marginally uniform on $[0, 1]$, but they are not independent in general.

Let $\mathcal{F}_a^b = \sigma(T_i : a \leq i \leq b)$. We use the following standard mixing coefficients:

$$\alpha_{\text{mix}}(r) := \sup_m \sup_{A \in \mathcal{F}_{-\infty}^m, B \in \mathcal{F}_{m+r}^\infty} |\mathbb{P}(B \cap A) - \mathbb{P}(A)\mathbb{P}(B)|$$

for strong, or α -, mixing,

$$\phi_{\text{mix}}(r) := \sup_m \sup_{\substack{A \in \mathcal{F}_{-\infty}^m, B \in \mathcal{F}_{m+r}^\infty \\ \mathbb{P}(A) > 0}} |\mathbb{P}(B | A) - \mathbb{P}(B)|$$

for ϕ -mixing, and

$$\beta_{\text{mix}}(r) := \sup_m \mathbb{E} \left[\sup_{B \in \mathcal{F}_{m+r}^\infty} |\mathbb{P}(B | \mathcal{F}_{-\infty}^m) - \mathbb{P}(B)| \right]$$

for absolute regularity, or β -mixing. Different normalizations of the β -mixing coefficient appear in the literature; only its role as a decoupling error is used below.

For fixed t , the event $\{T_{n+\ell} \leq t\}$ is separated from \mathcal{C}_n by ℓ time steps. Under ϕ -mixing this gives the direct conditional decoupling bound³

$$\sup_{t \in \mathbb{R}} |\mathbb{P}(T_{n+\ell} \leq t | \mathcal{C}_n) - F_T(t)| \leq \phi_{\text{mix}}(\ell) \quad \text{a.s.}$$

Evaluating this bound at the random threshold $T_{(k)}$, and setting

$$D_{n,k}^{(\ell)} := \mathbb{P}(T_{n+\ell} \leq T_{(k)} | \mathcal{C}_n),$$

3. Formally, we first apply the mixing bound on the countable set $t \in \mathbb{Q}$, choosing an almost-sure event on which all these inequalities hold. For a regular conditional distribution of $T_{n+\ell}$ given \mathcal{C}_n , the conditional c.d.f. is right-continuous in t ; since F_T is continuous, the bound extends from rational thresholds to all $t \in \mathbb{R}$. This almost-sure uniform version can then be evaluated at the random threshold $T_{(k)}$.

we obtain

$$\left| D_{n,k}^{(\ell)} - F_T(T_{(k)}) \right| \leq \phi_{\text{mix}}(\ell) \quad \text{a.s.}$$

Since $F_T(T_{(k)}) = U_{(k)}$, Proposition 4 and the triangle inequality give

$$W_1\left(\mathcal{L}(D_{n,k}^{(\ell)}), \beta_{n,k}\right) \leq \phi_{\text{mix}}(\ell) + W_1\left(\mathcal{L}(U_{(k)}), \beta_{n,k}\right).$$

The first term is the price of using a future dependent test point; the second is the deviation of the calibration order statistic from the i.i.d. beta reference.

A similar separation can be obtained for absolutely regular processes by blocking. Coupling lemmas for separated blocks, such as [Yu \(1994, Corollary 2.7\)](#), allow one to replace separated dependent blocks by independent copies at a cost controlled by the corresponding β -mixing coefficients. We do not need the explicit block construction in what follows. The relevant point is that, after the test-calibration dependence is handled by a direct ϕ -mixing argument, by a β -mixing blocking argument, or by an external independence assumption, the remaining problem is to control the calibration order statistic $U_{(k)}$.

We summarize the decoupling step by assuming that, for some deterministic $\Delta_\ell \geq 0$,

$$W_1\left(\mathcal{L}(D_{n,k}^{(\ell)}), \mathcal{L}(U_{(k)})\right) \leq \Delta_\ell.$$

For the direct ϕ -mixing argument above one may take $\Delta_\ell = \phi_{\text{mix}}(\ell)$; if the future test score has already been decoupled from the calibration block, then $\Delta_\ell = 0$. It remains to control $\mathcal{L}(U_{(k)})$. The external input we use is a Berry–Esseen theorem for sample quantiles of strongly mixing, equivalently α -mixing, sequences.

Theorem 16 (Berry–Esseen Bound for α -Mixing Sample Quantiles) *Let $(X_i)_{i \in \mathbb{Z}}$ be a stationary strongly mixing (α -mixing) sequence with marginal distribution function F . Fix $p \in (0, 1)$, write F^{-1} for the generalized inverse of F , and suppose that F has density f near $F^{-1}(p)$. Let*

$$F_n(x) := \frac{1}{n} \sum_{i=1}^n \mathbf{1}\{X_i \leq x\}.$$

We write F_n^{-1} for the generalized inverse of F_n . Assume the regularity conditions (C.1)–(C.5) of [Lahiri and Sun \(2009, Theorem, Section 2.3; see also Eq. \(1.4\)\)](#), including the strong-mixing rate condition on α_{mix} . Then

$$\sup_{x \in \mathbb{R}} \left| \mathbb{P}\left(\sqrt{n}\{F_n^{-1}(p) - F^{-1}(p)\} \leq x\right) - \Phi\left(\frac{x}{\tau_\infty(p)}\right) \right| = O(n^{-1/2}),$$

where

$$\tau_\infty^2(p) = \frac{\sigma_\infty^2(F^{-1}(p))}{f^2(F^{-1}(p))},$$

and

$$\sigma_\infty^2(F^{-1}(p)) = \sum_{j \in \mathbb{Z}} \text{Cov}\left(\mathbf{1}\{X_0 \leq F^{-1}(p)\}, \mathbf{1}\{X_j \leq F^{-1}(p)\}\right).$$

Suppose that the transformed calibration process $(U_i)_{i \in \mathbb{Z}}$ satisfies the assumptions of Theorem 16 at quantile level γ . Its marginal distribution is uniform, so $F^{-1}(\gamma) = \gamma$, $f(\gamma) = 1$, and, with the generalized inverse convention, $F_n^{-1}(\gamma) = U_{(\lceil n\gamma \rceil)}$. The conformal index $k_\gamma = \lceil (n+1)\gamma \rceil$ differs from $\lceil n\gamma \rceil$ by at most one, so the same Berry–Esseen approximation applies to $U_{(k_\gamma)}$, with the index perturbation absorbed in the $O(n^{-1/2})$ remainder. Thus the Berry–Esseen assumption in Proposition 15 holds for k_γ with $a_n = O(n^{-1/2})$ and

$$\tau_\gamma^2 = \gamma(1-\gamma) + 2 \sum_{j \geq 1} \text{Cov}(\mathbf{1}\{U_0 \leq \gamma\}, \mathbf{1}\{U_j \leq \gamma\}),$$

whenever the covariance series is well defined and $\tau_\gamma^2 > 0$. Therefore,

$$W_1\left(\mathcal{L}(D_{n,k_\gamma}^{(\ell)}), \beta_{n,k_\gamma}\right) \leq \Delta_\ell + \sqrt{\frac{2}{\pi n}} \left| \tau_\gamma - \sqrt{\gamma(1-\gamma)} \right| + O(n^{-1/2}). \quad (1)$$

Thus Theorem 11, together with $|k_\gamma/(n+1) - \gamma| \leq 1/(n+1)$, gives the marginal coverage bound

$$|\mathbb{P}(T_{n+\ell} \leq T_{(k_\gamma)}) - \gamma| \leq \Delta_\ell + \sqrt{\frac{2}{\pi n}} \left| \tau_\gamma - \sqrt{\gamma(1-\gamma)} \right| + O(n^{-1/2}).$$

Theorem 12 gives the corresponding bad-calibration statement from the same radius. Let

$$\rho_{n,\ell} := W_1\left(\mathcal{L}(D_{n,k_\gamma}^{(\ell)}), \beta_{n,k_\gamma}\right).$$

The Wasserstein bound above shows that

$$\rho_{n,\ell} \leq \Delta_\ell + \sqrt{\frac{2}{\pi n}} \left| \tau_\gamma - \sqrt{\gamma(1-\gamma)} \right| + O(n^{-1/2}).$$

Applied with $p = 1$, Theorem 12 gives that for every $t \in [0, 1]$ and every $\varepsilon > 0$,

$$\mathbb{P}\left(D_{n,k_\gamma}^{(\ell)} \leq t\right) \leq \mathbb{P}\left(B_{n,k_\gamma} \leq t + \varepsilon\right) + \frac{\rho_{n,\ell}}{\varepsilon}, \quad B_{n,k_\gamma} \sim \beta_{n,k_\gamma}.$$

In particular, for any $\eta \in (0, \gamma)$,

$$\mathbb{P}\left(D_{n,k_\gamma}^{(\ell)} \leq \gamma - \eta\right) \leq \mathbb{P}\left(B_{n,k_\gamma} \leq \gamma - \eta/2\right) + \frac{2\rho_{n,\ell}}{\eta}.$$

Thus the probability of a low realized-coverage event is controlled by the i.i.d. beta lower tail, plus the decoupling and Berry–Esseen errors encoded in $\rho_{n,\ell}$.

4.3.1. EXAMPLE: AR(1) PROCESS

Let $(T_i)_{i \in \mathbb{Z}}$ be a stationary AR(1) process,

$$T_i = aT_{i-1} + \varepsilon_i, \quad \varepsilon_i \stackrel{\text{iid}}{\sim} N(0, 1 - a^2), \quad |a| < 1.$$

Then $T_i \sim N(0, 1)$ for every i , but the scores are serially dependent. The calibration sample is $\mathcal{C}_n = (T_1, \dots, T_n)$, and the test score is $T_{n+\ell}$ for a fixed horizon $\ell \geq 1$. By the Markov property,

$$T_{n+\ell} | \mathcal{C}_n \sim N(a^\ell T_n, 1 - a^{2\ell}).$$

Therefore the realized coverage at threshold $T_{(k)}$ is

$$D_{n,k}^{(\ell)} = \mathbb{P}(T_{n+\ell} \leq T_{(k)} \mid \mathcal{C}_n) = \Phi\left(\frac{T_{(k)} - a^\ell T_n}{\sqrt{1 - a^{2\ell}}}\right). \quad (2)$$

For this example, the decoupling radius Δ_ℓ in (1) can be obtained directly from the Markov property without invoking mixing conditions: since $T_{n+\ell} \mid \mathcal{C}_n \sim N(a^\ell T_n, 1 - a^{2\ell})$ differs from $N(0, 1)$ only through a mean shift of order $|a|^\ell$, one obtains $\Delta_\ell \lesssim |a|^\ell$. The geometric decay used below thus arises from the Markov structure of the AR(1) alone.

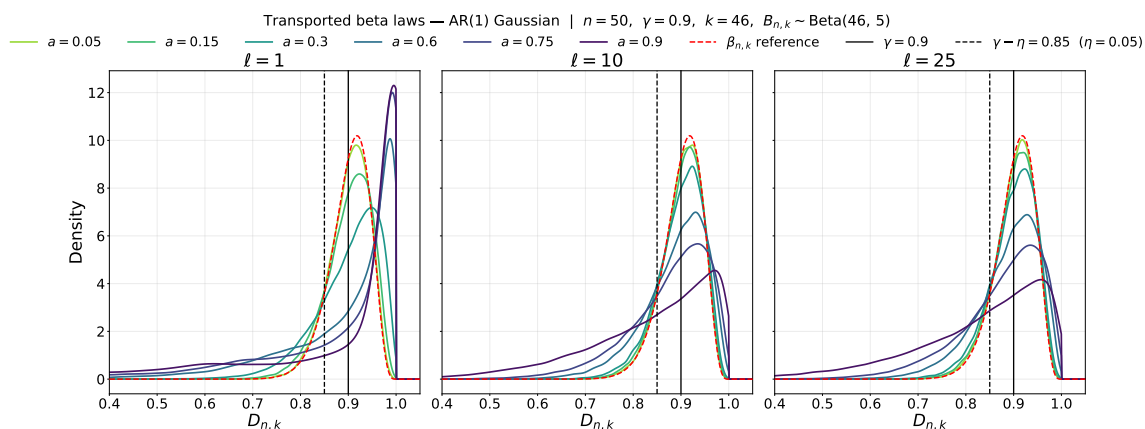


Figure 4: Realized-coverage laws $\nu_{n,k}$ for the Gaussian AR(1) model with $n = 50$ and $\gamma = 0.9$, against the i.i.d. beta reference $\beta_{n,k}$ (dashed red). At $\ell = 1$, larger positive values of a produce a more dispersed realized-coverage law, with both a sharper concentration near 1 and a heavier left tail extending below the bad-calibration threshold $\gamma - \eta = 0.85$. As ℓ grows, the direct test-calibration dependence weakens and the laws approach the calibration-order-statistic law $\mathcal{L}(U_{(k)})$; this limit equals $\beta_{n,k}$ only when the calibration scores are independent.

The expression contains two effects. The order statistic $T_{(k)}$ is the calibration contribution, while $a^\ell T_n$ is the remaining dependence between the future test score and the last calibration score. As ℓ increases, a^ℓ decreases geometrically and the test score becomes closer to an independent draw from the marginal $N(0, 1)$. In the limit $\ell \rightarrow \infty$,

$$D_{n,k}^{(\ell)} \rightarrow \Phi(T_{(k)}) = U_{(k)}$$

in distribution. The remaining deviation from the beta reference is then the calibration-order-statistic effect controlled by the α -mixing Berry–Esseen argument above.

Figure 4 shows the induced realized-coverage laws for fixed $n = 50$ and $\gamma = 0.9$, across several values of a and $\ell \in \{1, 10, 25\}$. Larger a and smaller ℓ produce stronger test-calibration effects; increasing ℓ removes this contribution and moves the law toward the calibration-order-statistic law $U_{(k)}$, which may still differ from the beta benchmark when calibration dependence is strong.

The complementary roles of ℓ and n for the AR(1) example are illustrated in Figures 6, 7 and 8 in Appendix B.2. Figure 6 displays the Monte Carlo estimate of $W_1(\nu_{n,k_\gamma}, \beta_{n,k_\gamma})$ and the bound (1) as functions of the horizon ℓ , for fixed $n = 200$ and $a \in \{0, 0.3, 0.6, 0.9\}$. For $a = 0$ the scores are i.i.d. and W_1 is negligible for all ℓ . For $a > 0$, the test-calibration term $|a|^\ell$ decays geometrically, and both quantities flatten as ℓ grows: the bound flattens at the Berry–Esseen floor $\sqrt{2/(\pi n)} |\tau_\gamma - \sqrt{\gamma(1-\gamma)}|$, while W_1 flattens at the (typically smaller) limiting value $W_1(\mathcal{L}(U_{(k_\gamma)}), \beta_{n,k_\gamma})$ associated with the calibration order statistic alone.

Figure 7 fixes $\ell \in \{1, 10, 25\}$ and varies n . The Monte Carlo curves confirm the marginal-coverage gap inequality of Theorem 11, $|\text{Cov}(k_\gamma) - k_\gamma/(n+1)| \leq W_1$. The asymptotic upper bound on W_1 , on the other hand, is informative only once n is large enough relative to a and ℓ for the Berry–Esseen approximation to take effect: it is conservative for small n combined with large a and small ℓ (top-right panels), and becomes tighter once $|a|^\ell$ is small, so that the bound and W_1 are jointly dominated by the Berry–Esseen calibration term.

Finally, Figure 8 translates these Wasserstein distances into bad-calibration probabilities through Theorem 12: the Markov-type tail control $\mathbb{P}(B_{n,k_\gamma} \leq \gamma - \eta/2) + 2W_1/\eta$ is loose, and may exceed one, whenever W_1 is comparable to or larger than η ; it tightens progressively as ℓ increases and the test-dependence contribution to W_1 decays.

5. Conclusion

We introduced a transported-beta perspective on split conformal prediction. Instead of viewing conformal validity only through marginal coverage, we studied the law of the calibration-conditional coverage induced by the realized calibration sample. In the continuous i.i.d. case this law is exactly $\text{Beta}(k, n+1-k)$, so the classical split conformal coverage level is recovered as its mean, while its lower tail quantifies bad-calibration events.

The main message is that this beta law remains a useful finite-sample reference beyond the i.i.d. setting. By comparing the realized-coverage law $\nu_{n,k}$ with the beta benchmark $\beta_{n,k}$ on the coverage scale, Wasserstein distances give direct control of marginal coverage gaps and bad-calibration probabilities. This formulation separates different mechanisms of non-i.i.d. behavior: test-side distribution shift transports the beta law through a deterministic coverage map, whereas calibration dependence changes the order-statistic law itself.

The examples illustrate how this viewpoint can be used as a diagnostic and comparison tool rather than as a single new conformal algorithm. In scale-shift models the deformation is explicit and the Wasserstein bound can be sharp; in clustered and mixing settings the distance to the beta reference captures effective sample size and dependence effects. Simulations on dependent uniform processes confirm that the Berry–Esseen approximation tracks the empirical Wasserstein distance closely, even at moderate sample sizes. Future work could focus on estimating the transported-beta radius from data, extending the framework to adaptive or weighted conformal procedures, and developing sharper finite-sample tail comparisons.

References

- Luigi Ambrosio, Nicola Gigli, and Giuseppe Savaré. *Gradient Flows in Metric Spaces and in the Space of Probability Measures*. Birkhäuser, Basel, 2005.
- Anastasios N. Angelopoulos and Stephen Bates. A gentle introduction to conformal prediction and distribution-free uncertainty quantification, 2021.
- Liviu Aolaritei, Zheyu Oliver Wang, Julie Zhu, Michael I. Jordan, and Youssef Marzouk. Conformal prediction under Lévy–Prokhorov distribution shifts: Robustness to local and global perturbations, 2025.
- Rina Foygel Barber, Emmanuel J. Candès, Aaditya Ramdas, and Ryan J. Tibshirani. Conformal prediction beyond exchangeability. *The Annals of Statistics*, 51(2):816–845, 2023. doi: 10.1214/23-AOS2276.
- Alvaro H. C. Correia and Christos Louizos. Non-exchangeable conformal prediction with optimal transport: Tackling distribution shifts with unlabeled data. In *The Thirty-ninth Annual Conference on Neural Information Processing Systems*, 2025.
- Ulysse Gazin. Asymptotics for conformal inference. *arXiv preprint arXiv:2409.12019*, 2024.
- Ulysse Gazin, Gilles Blanchard, and Etienne Roquain. Transductive conformal inference with adaptive scores. In *Proceedings of the 27th International Conference on Artificial Intelligence and Statistics (AISTATS)*, volume 238 of *Proceedings of Machine Learning Research*, pages 1504–1512, 2024.
- S. N. Lahiri and S. Sun. A berry–esseen theorem for sample quantiles under weak dependence. *The Annals of Applied Probability*, 19(1):108–126, 2009. doi: 10.1214/08-AAP533.
- Jing Lei and Larry Wasserman. Distribution-free prediction bands for non-parametric regression. *Journal of the Royal Statistical Society: Series B (Statistical Methodology)*, 76(1):71–96, 2014. doi: 10.1111/rssb.12021.
- Paulo C. Marques F. Universal distribution of the empirical coverage in split conformal prediction. *Statistics and Probability Letters*, 219:110350, 2025. doi: 10.1016/j.spl.2024.110350.
- Roberto I Oliveira, Paulo Orenstein, Thiago Ramos, and Joao Vitor Romano. Split conformal prediction and non-exchangeable data. *Journal of Machine Learning Research*, 25(225):1–38, 2024.
- Harris Papadopoulos, Kostas Proedrou, Volodya Vovk, and Alex Gammerman. Inductive confidence machines for regression. In Tapio Elomaa, Heikki Mannila, and Hannu Toivonen, editors, *Machine Learning: ECML 2002*, volume 2430 of *Lecture Notes in Computer Science*, pages 345–356, Berlin, Heidelberg, 2002. Springer. doi: 10.1007/3-540-36755-1.29.
- Gabriel Peyré and Marco Cuturi. Computational optimal transport. *Foundations and Trends in Machine Learning*, 11(5–6):355–607, 2019. doi: 10.1561/22000000073.

- Filippo Santambrogio. *Optimal Transport for Applied Mathematicians*, volume 87 of *Progress in Nonlinear Differential Equations and Their Applications*. Birkhäuser, Cham, 2015. doi: 10.1007/978-3-319-20828-2.
- Cédric Villani. *Optimal Transport: Old and New*, volume 338 of *Grundlehren der mathematischen Wissenschaften*. Springer, Berlin, Heidelberg, 2009. doi: 10.1007/978-3-540-71050-9.
- Vladimir Vovk. Conditional Validity of Inductive Conformal Predictors. In *Proceedings of the Asian Conference on Machine Learning*, pages 475–490. PMLR, November 2012. URL <https://proceedings.mlr.press/v25/vovk12.html>.
- Vladimir Vovk, Alex Gammerman, and Glenn Shafer. *Algorithmic Learning in a Random World*. Springer-Verlag, Berlin, Heidelberg, 2005. ISBN 0387001522.
- Rui Xu, Chao Chen, Yue Sun, Parvathinathan Venkitasubramaniam, and Sihong Xie. Wasserstein-regularized conformal prediction under general distribution shift. In *The Thirteenth International Conference on Learning Representations*, 2025.
- Bin Yu. Rates of convergence for empirical processes of stationary mixing sequences. *The Annals of Probability*, 22(1):94–116, 1994. doi: 10.1214/aop/1176988849.

Appendix A. Proofs

A.1. Proof of Proposition 2

Proof Conditional on the calibration sample S_1, \dots, S_n , the order statistic $S_{(k)}$ is fixed. Since S_{n+1} is independent of the calibration sample and has distribution F_S , the conditional coverage is simply the distribution function evaluated at the realized threshold:

$$C_{n,k} = \mathbb{P}(S_{n+1} \leq S_{(k)} \mid S_1, \dots, S_n) = F_S(S_{(k)}).$$

The remaining step is to identify the distribution of this random value as the calibration sample varies. Define

$$U_i = F_S(S_i), \quad i = 1, \dots, n.$$

By the probability integral transform, the variables U_1, \dots, U_n are i.i.d. $\text{Unif}(0, 1)$. Since F_S is monotone, the ordering of the S_i 's is preserved, and hence

$$F_S(S_{(k)}) = U_{(k)}.$$

The k -th order statistic of n i.i.d. uniform random variables has distribution

$$U_{(k)} \sim \text{Beta}(k, n + 1 - k).$$

Therefore,

$$C_{n,k} = F_S(S_{(k)}) \sim \text{Beta}(k, n + 1 - k).$$

■

A.2. Proof of Theorem 11

Proof The i.i.d. reference law satisfies

$$\mathbb{E}_{Z \sim \beta_{n,k}} [Z] = \frac{k}{n+1}.$$

On the other hand, by the tower property,

$$\text{Cov}(k) = \mathbb{E}[D_{n,k}] = \mathbb{E}_{Z \sim \nu_{n,k}} [Z].$$

Therefore the marginal coverage gap is

$$\left| \text{Cov}(k) - \frac{k}{n+1} \right| = \left| \mathbb{E}_{Z \sim \nu_{n,k}} [Z] - \mathbb{E}_{Z \sim \beta_{n,k}} [Z] \right|.$$

By Proposition 6,

$$\left| \mathbb{E}_{Z \sim \nu_{n,k}} [Z] - \mathbb{E}_{Z \sim \beta_{n,k}} [Z] \right| \leq W_1(\nu_{n,k}, \beta_{n,k}),$$

which proves the first claim.

If $\nu_{n,k} \in \mathcal{B}_p(\beta_{n,k}, \rho)$, then Proposition 5 gives

$$W_1(\nu_{n,k}, \beta_{n,k}) \leq W_p(\nu_{n,k}, \beta_{n,k}) \leq \rho.$$

This proves the beta-neighborhood bound.

If $k_\gamma = \lceil (n+1)\gamma \rceil \leq n$, then

$$\frac{k_\gamma}{n+1} \geq \gamma$$

and

$$0 \leq \frac{k_\gamma}{n+1} - \gamma \leq \frac{1}{n+1}.$$

The lower bound and the final absolute-error bound follow immediately from the beta-neighborhood bound and the discretization bound above. \blacksquare

A.3. Proof of Theorem 12

Proof Let $B_{n,k} \sim \beta_{n,k}$, and let

$$T_{\text{mon}} = F_{\nu_{n,k}}^{-1} \circ F_{\beta_{n,k}}$$

be the monotone transport map from $\beta_{n,k}$ to $\nu_{n,k}$. Define

$$D_{n,k}^* := T_{\text{mon}}(B_{n,k}).$$

By Proposition 7, $D_{n,k}^* \sim \nu_{n,k}$. Therefore $D_{n,k}^* \stackrel{d}{=} D_{n,k}$, and

$$\mathbb{P}(D_{n,k} \leq t) = \mathbb{P}(T_{\text{mon}}(B_{n,k}) \leq t).$$

Define

$$G_\varepsilon := \{|T_{\text{mon}}(B_{n,k}) - B_{n,k}| \leq \varepsilon\}.$$

On G_ε , if $T_{\text{mon}}(B_{n,k}) \leq t$, then

$$B_{n,k} \leq T_{\text{mon}}(B_{n,k}) + \varepsilon \leq t + \varepsilon.$$

Thus

$$\{T_{\text{mon}}(B_{n,k}) \leq t\} \cap G_\varepsilon \subseteq \{B_{n,k} \leq t + \varepsilon\}.$$

It follows that

$$\mathbb{P}(D_{n,k} \leq t) \leq \mathbb{P}(B_{n,k} \leq t + \varepsilon) + \mathbb{P}(G_\varepsilon^c).$$

By Markov's inequality and the optimality of T_{mon} ,

$$\begin{aligned} \mathbb{P}(G_\varepsilon^c) &= \mathbb{P}(|T_{\text{mon}}(B_{n,k}) - B_{n,k}| > \varepsilon) \\ &\leq \frac{\mathbb{E}[|T_{\text{mon}}(B_{n,k}) - B_{n,k}|^p]}{\varepsilon^p} \\ &= \frac{W_p^p(\nu_{n,k}, \beta_{n,k})}{\varepsilon^p} \leq \left(\frac{\rho}{\varepsilon}\right)^p. \end{aligned}$$

Combining the last two displays proves the claim. \blacksquare

A.4. Proof of Proposition 13

Proof Since \tilde{T} is independent of \mathcal{C}_n , conditioning on the calibration sample fixes $T_{(k)}$ and gives

$$D_{n,k} = \mathbb{P}\left(\tilde{T} \leq T_{(k)} \mid \mathcal{C}_n\right) = F_{\tilde{T}}(T_{(k)}).$$

This proves the first display.

Now suppose that the calibration scores have common continuous marginal distribution function F_T , and define $U_i = F_T(T_i)$. By the probability integral transform, each U_i is marginally uniform on $[0, 1]$; no independence among the U_i 's is required for this marginal statement. Since F_T is monotone, the ordering is preserved, so

$$F_T(T_{(k)}) = U_{(k)}.$$

With the generalized inverse convention, this gives

$$F_{\tilde{T}}(T_{(k)}) \stackrel{d}{=} F_{\tilde{T}}(F_T^{-1}(U_{(k)})) = h(U_{(k)}), \quad h := F_{\tilde{T}} \circ F_T^{-1}.$$

Therefore

$$\nu_{n,k} = \mathcal{L}(D_{n,k}) = h_{\#}\mathcal{L}(U_{(k)}).$$

In the i.i.d. uniform reference case, the order statistic satisfies $U_{(k)} \sim \beta_{n,k}$, and the final display follows. \blacksquare

A.5. Proof of Proposition 14

Proof The event $U_{(k)} \leq t$ is exactly the event that at least k calibration variables are at most t , which gives the first identity. For the i.i.d. uniform reference sample, the corresponding count is $\text{Bin}(n, t)$, and its k -th order statistic has law $\beta_{n,k}$. The Wasserstein identity then follows from Proposition 8. \blacksquare

A.6. Details for the Half-Normal Scale-Shift Example

For $\sigma > 0$, the distribution function of $|N(0, \sigma^2)|$ is

$$F_{\sigma}(t) = 2\Phi(t/\sigma) - 1, \quad t \geq 0.$$

Hence

$$F_{\sigma}^{-1}(u) = \sigma \Phi^{-1}\left(\frac{u+1}{2}\right), \quad 0 < u < 1.$$

Writing

$$q(u) := \Phi^{-1}\left(\frac{u+1}{2}\right),$$

we have $F_{\sigma}^{-1}(u) = \sigma q(u)$. Therefore the calibration-to-test transport map is

$$\begin{aligned} F_{\sigma_{\tilde{T}}}(F_{\sigma_T}^{-1}(u)) &= F_{\sigma_{\tilde{T}}}(\sigma_T q(u)) \\ &= 2\Phi\left(\frac{\sigma_T}{\sigma_{\tilde{T}}}q(u)\right) - 1 \\ &= 2\Phi\left(\frac{q(u)}{r}\right) - 1 = h_r(u), \end{aligned}$$

where $r = \sigma_{\tilde{T}}/\sigma_T$.

Let

$$B_{n,k} := F_{\sigma_T}(T_{(k)}).$$

Since the calibration sample is i.i.d. from F_{σ_T} ,

$$B_{n,k} \sim \text{Beta}(k, n + 1 - k) = \beta_{n,k}.$$

Moreover,

$$\begin{aligned} D_{n,k} &= \mathbb{P}\left(\tilde{T} \leq T_{(k)} \mid T_1, \dots, T_n\right) \\ &= F_{\sigma_{\tilde{T}}}(T_{(k)}) \\ &= F_{\sigma_{\tilde{T}}}\left(F_{\sigma_T}^{-1}(B_{n,k})\right) \\ &= h_r(B_{n,k}). \end{aligned}$$

Thus

$$\nu_{n,k}^{(r)} = \mathcal{L}(D_{n,k}) = (h_r)_{\#}\beta_{n,k},$$

and

$$\text{Cov}(k) = \mathbb{E}[h_r(B_{n,k})].$$

We next derive the density of the transported law. Let $z \in (0, 1)$. If $z = h_r(u)$, then

$$z = 2\Phi\left(\frac{q(u)}{r}\right) - 1.$$

Therefore,

$$\Phi^{-1}\left(\frac{z+1}{2}\right) = \frac{q(u)}{r},$$

and hence

$$q(u) = rq(z).$$

It follows that

$$h_r^{-1}(z) = 2\Phi(rq(z)) - 1.$$

Differentiating with respect to z ,

$$\frac{d}{dz}h_r^{-1}(z) = 2\phi(rq(z))r q'(z).$$

Since

$$q(z) = \Phi^{-1}\left(\frac{z+1}{2}\right),$$

we have

$$q'(z) = \frac{1}{2\phi(q(z))}.$$

Therefore,

$$\frac{d}{dz}h_r^{-1}(z) = r \frac{\phi(rq(z))}{\phi(q(z))}.$$

If $f_{n,k}$ denotes the density of $\beta_{n,k} = \text{Beta}(k, n+1-k)$, then the density of $D_{n,k} = h_r(B_{n,k})$ is

$$\begin{aligned} f_{D,r}(z) &= f_{n,k}(h_r^{-1}(z)) \left| \frac{d}{dz} h_r^{-1}(z) \right| \\ &= f_{n,k}(2\Phi(rq(z)) - 1) r \frac{\phi(rq(z))}{\phi(q(z))}, \quad 0 < z < 1. \end{aligned}$$

We now justify the sharpness of the Wasserstein bound in this example. The map h_r is increasing on $(0, 1)$. Moreover, since $q(u) > 0$ for $u \in (0, 1)$,

$$r > 1 \implies h_r(u) < u, \quad r < 1 \implies h_r(u) > u.$$

Thus $h_r - \text{id}$ has constant sign on $(0, 1)$. The monotone coupling $(B_{n,k}, h_r(B_{n,k}))$ is optimal in one dimension, and therefore

$$\begin{aligned} W_1(\nu_{n,k}^{(r)}, \beta_{n,k}) &= \mathbb{E}[|h_r(B_{n,k}) - B_{n,k}|] \\ &= |\mathbb{E}[h_r(B_{n,k}) - B_{n,k}]| \\ &= \left| \text{Cov}(k) - \frac{k}{n+1} \right|. \end{aligned}$$

The last equality uses $\mathbb{E}[B_{n,k}] = k/(n+1)$.

Finally, we derive the local small-shift approximation. Write $r = e^\delta$. Then

$$h_{e^\delta}(u) = 2\Phi(e^{-\delta}q(u)) - 1.$$

Differentiating with respect to δ ,

$$\frac{\partial}{\partial \delta} h_{e^\delta}(u) = -2e^{-\delta} \phi(e^{-\delta}q(u))q(u).$$

At $\delta = 0$,

$$\left. \frac{\partial}{\partial \delta} h_{e^\delta}(u) \right|_{\delta=0} = -2\phi(q(u))q(u).$$

Thus

$$h_{e^\delta}(u) = u - 2\delta \phi(q(u))q(u) + O(\delta^2).$$

Taking expectations under $B_{n,k} \sim \beta_{n,k}$ gives

$$\text{Cov}(k) = \frac{k}{n+1} - 2\delta \mathbb{E}[\phi(q(B_{n,k}))q(B_{n,k})] + O(\delta^2).$$

For $k_\gamma = \lceil (n+1)\gamma \rceil$, the beta law concentrates around γ . Therefore,

$$\mathbb{E}[\phi(q(B_{n,k_\gamma}))q(B_{n,k_\gamma})] = \phi(q(\gamma))q(\gamma) + O(n^{-1}),$$

and hence

$$\text{Cov}(k_\gamma) - \gamma = -2\delta \phi(q(\gamma))q(\gamma) + O(\delta^2) + O(n^{-1}).$$

A.7. Proof of Proposition 15

Proof Write

$$s_\gamma := \sqrt{\gamma(1-\gamma)}.$$

Let $B_{n,k_\gamma} \sim \beta_{n,k_\gamma}$, and denote by F_U and F_B the distribution functions of $U_{(k_\gamma)}$ and B_{n,k_γ} , respectively. Since both laws are supported on $[0, 1]$, Proposition 8 gives

$$W_1(\mathcal{L}(U_{(k_\gamma)}), \beta_{n,k_\gamma}) = \int_0^1 |F_U(t) - F_B(t)| dt.$$

We now rewrite the two distribution functions on the central-limit scale. For $x \in \mathbb{R}$, set

$$\begin{aligned} A_n(x) &:= \mathbb{P}(\sqrt{n}\{U_{(k_\gamma)} - \gamma\} \leq x), \\ A_n^0(x) &:= \mathbb{P}(\sqrt{n}\{B_{n,k_\gamma} - \gamma\} \leq x). \end{aligned}$$

By assumption,

$$\sup_{x \in \mathbb{R}} \left| A_n(x) - \Phi\left(\frac{x}{\tau_\gamma}\right) \right| \leq a_n.$$

For the i.i.d. beta benchmark, the classical Berry–Esseen theorem for sample quantiles gives

$$\sup_{x \in \mathbb{R}} \left| A_n^0(x) - \Phi\left(\frac{x}{s_\gamma}\right) \right| \leq c_n, \quad c_n = O(n^{-1/2}).$$

This is the standard Berry–Esseen approximation for the k_γ -th order statistic of an i.i.d. uniform sample. Since $k_\gamma = \lceil (n+1)\gamma \rceil$, we have $k_\gamma/(n+1) = \gamma + O(n^{-1})$; this centering difference is absorbed by the $O(n^{-1/2})$ remainder.

Now fix $t \in [0, 1]$. Then

$$F_U(t) = A_n(\sqrt{n}(t - \gamma)), \quad F_B(t) = A_n^0(\sqrt{n}(t - \gamma)).$$

Using the triangle inequality inside the integral,

$$\begin{aligned} |F_U(t) - F_B(t)| &\leq \left| A_n(\sqrt{n}(t - \gamma)) - \Phi\left(\frac{\sqrt{n}(t - \gamma)}{\tau_\gamma}\right) \right| \\ &\quad + \left| \Phi\left(\frac{\sqrt{n}(t - \gamma)}{\tau_\gamma}\right) - \Phi\left(\frac{\sqrt{n}(t - \gamma)}{s_\gamma}\right) \right| \\ &\quad + \left| \Phi\left(\frac{\sqrt{n}(t - \gamma)}{s_\gamma}\right) - A_n^0(\sqrt{n}(t - \gamma)) \right|. \end{aligned}$$

Integrating over $t \in [0, 1]$ and using the two uniform Berry–Esseen bounds therefore yields

$$W_1(\mathcal{L}(U_{(k_\gamma)}), \beta_{n,k_\gamma}) \leq a_n + c_n + I_n,$$

where

$$I_n := \int_0^1 \left| \Phi\left(\frac{\sqrt{n}(t - \gamma)}{\tau_\gamma}\right) - \Phi\left(\frac{\sqrt{n}(t - \gamma)}{s_\gamma}\right) \right| dt.$$

It remains to identify I_n . With the change of variables $x = \sqrt{n}(t - \gamma)$,

$$\begin{aligned} I_n &= \frac{1}{\sqrt{n}} \int_{-\sqrt{n}\gamma}^{\sqrt{n}(1-\gamma)} \left| \Phi\left(\frac{x}{\tau_\gamma}\right) - \Phi\left(\frac{x}{s_\gamma}\right) \right| dx \\ &\leq \frac{1}{\sqrt{n}} \int_{\mathbb{R}} \left| \Phi\left(\frac{x}{\tau_\gamma}\right) - \Phi\left(\frac{x}{s_\gamma}\right) \right| dx. \end{aligned}$$

The functions $x \mapsto \Phi(x/\tau_\gamma)$ and $x \mapsto \Phi(x/s_\gamma)$ are the distribution functions of $N(0, \tau_\gamma^2)$ and $N(0, s_\gamma^2)$. Thus the one-dimensional W_1 formula on \mathbb{R} gives

$$\int_{\mathbb{R}} \left| \Phi\left(\frac{x}{\tau_\gamma}\right) - \Phi\left(\frac{x}{s_\gamma}\right) \right| dx = W_1(N(0, \tau_\gamma^2), N(0, s_\gamma^2)).$$

By Lemma 9,

$$W_1(N(0, \tau_\gamma^2), N(0, s_\gamma^2)) = \sqrt{\frac{2}{\pi}} |\tau_\gamma - s_\gamma|.$$

Consequently,

$$I_n \leq \sqrt{\frac{2}{\pi n}} \left| \tau_\gamma - \sqrt{\gamma(1-\gamma)} \right|.$$

Combining this with $c_n = O(n^{-1/2})$ gives

$$W_1(\mathcal{L}(U_{(k_\gamma)}), \beta_{n,k_\gamma}) \leq a_n + \sqrt{\frac{2}{\pi n}} \left| \tau_\gamma - \sqrt{\gamma(1-\gamma)} \right| + O(n^{-1/2}),$$

which is the first claim. If $a_n = O(n^{-1/2})$, then the term a_n is absorbed into the final remainder, giving the second display. \blacksquare

Appendix B. Example additional results

This section presents additional illustrations for the two worked examples in the main text. In both cases, $W_1(\nu_{n,k}, \beta_{n,k})$, the coverage gap and the transported laws $\nu_{n,k}$ are estimated via Monte Carlo with 50,000 simulations per configuration, by drawing directly from the underlying process in each example and computing the relevant quantities empirically. Shaded bands throughout indicate ± 2 standard errors across simulations. In general, standard errors are very low; the wider band for the coverage gap observed in Figure 7 near zero is a consequence of the logarithmic scale employed, as the absolute error remains stable while the gap itself approaches zero.

B.1. Half-normal illustrations and results

Figure 5 complements the density plot in the main text by showing the full CDF deformation across a wider range of r and n . The left panels make the shaded W_1 area directly visible for each (r, n) pair, confirming that the deformation is stable across calibration sizes. The right panel traces W_1 and the coverage gap jointly as functions of r , verifying the exact equality from both sides of $r = 1$ and across all three values of n .

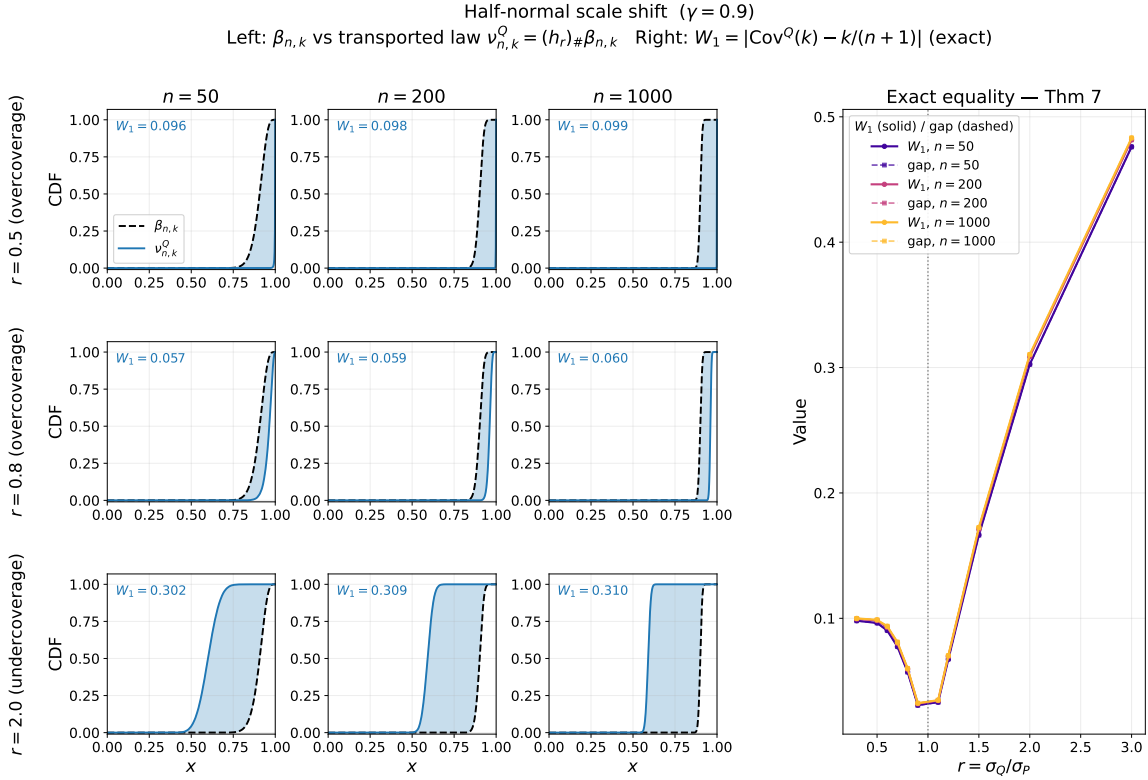


Figure 5: Half-normal scale-shift example with $\gamma = 0.9$. **Left:** CDFs of $\nu_{n,k}^{(r)} = (h_r)_{\#}\beta_{n,k}$ (solid blue) against $\beta_{n,k}$ (dashed black) for $r \in \{0.5, 0.8, 2.0\}$ and $n \in \{50, 200, 1000\}$; the shaded area equals $W_1(\nu_{n,k}^{(r)}, \beta_{n,k})$ and is essentially constant across n . **Right:** exact identity $W_1(\nu_{n,k}^{(r)}, \beta_{n,k}) = |\text{Cov}(k) - k/(n+1)|$ verified across $r \in [0.3, 3.0]$; the asymmetry around $r = 1$ reflects the nonlinearity of h_r , with undercoverage ($r > 1$) incurring a larger transport cost than overcoverage ($r < 1$) for the same $|r - 1|$.

B.2. AR(1) illustrations and results

Figures 6, 7, and 8 complement Figure 4 by quantifying the deformation across a wider range of configurations. Figure 6 traces W_1 and the bound (1) as functions of ℓ for fixed $n = 200$, showing the geometric decay and the residual Berry–Esseen floor. Figure 7 varies n for fixed $\ell \in \{1, 10, 25\}$, confirming the chain coverage gap $\leq W_1 \leq$ Berry–Esseen bound across all configurations. Figure 8 translates these into bad-calibration probabilities, with the bound tightening as ℓ increases.

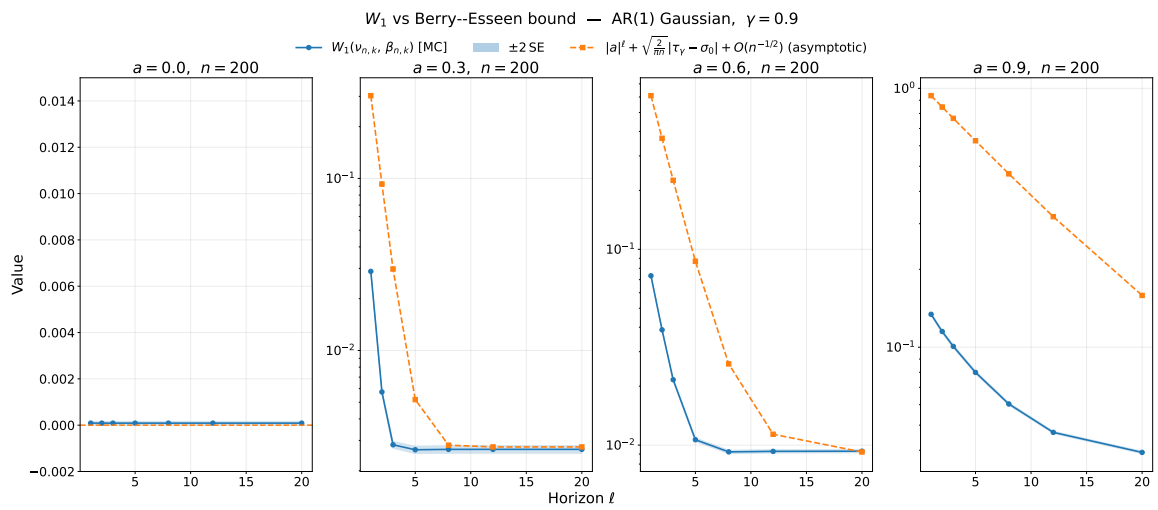


Figure 6: $W_1(\nu_{n,k,\gamma}, \beta_{n,k,\gamma})$ (solid blue) and the asymptotic bound (1) (dashed orange) as functions of ℓ , for $n = 200$, $\gamma = 0.9$, and $a \in \{0, 0.3, 0.6, 0.9\}$. For $a = 0$, W_1 is negligible for all ℓ ; for $a > 0$, both decay geometrically and level off at the Berry–Esseen floor, which depends only on n and the long-run variance τ_γ^2 .

Bound comparisons — AR(1) Gaussian, $\gamma = 0.9$
 gap (dashed) $\leq W_1$ (solid) \leq Berry--Esseen bound (dotted, asymptotic)

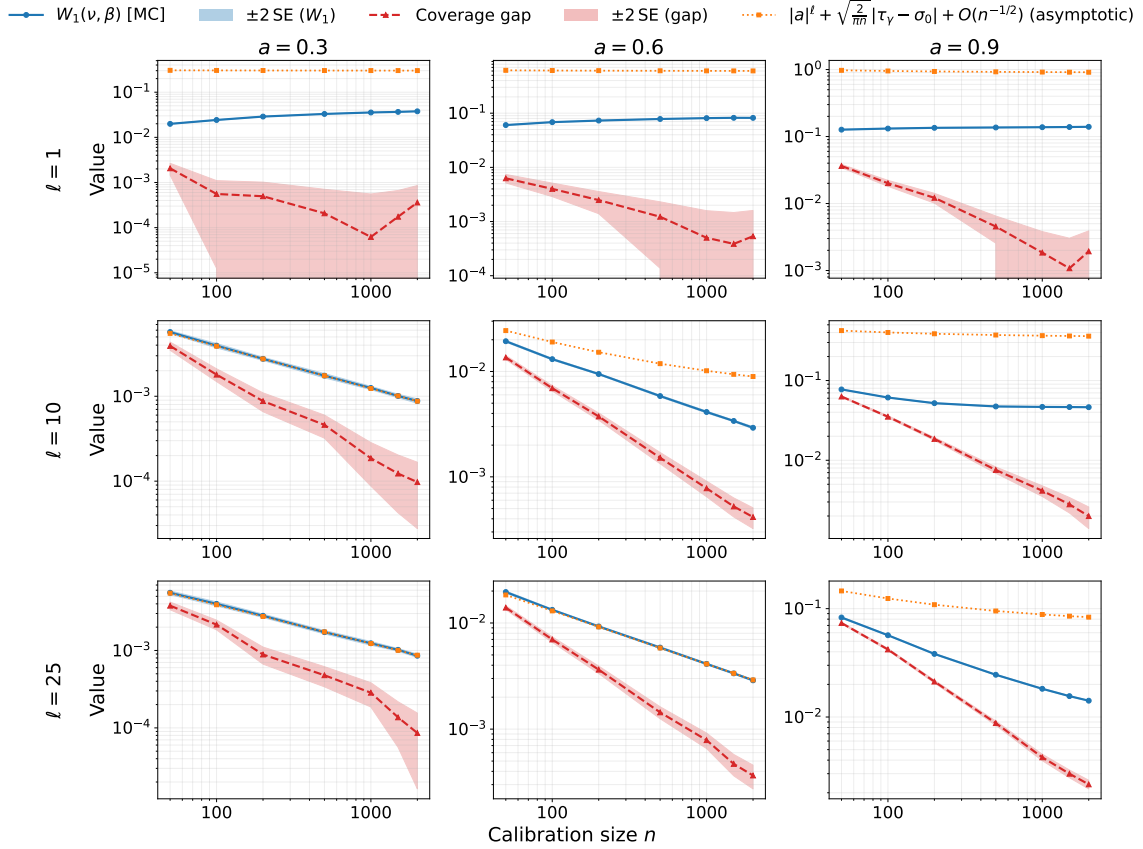


Figure 7: Chain of bounds $|\text{Cov}(k_\gamma) - k_\gamma/(n+1)| \leq W_1(\nu_{n,k_\gamma}, \beta_{n,k_\gamma}) \leq |a|^\ell + \sqrt{2/(\pi n)} |\tau_\gamma - \sqrt{\gamma(1-\gamma)}| + O(n^{-1/2})$ as a function of n , for $\gamma = 0.9$, $a \in \{0.3, 0.6, 0.9\}$, and $\ell \in \{1, 10, 25\}$. Solid blue: Monte-Carlo W_1 ; dashed red: coverage gap; dotted orange: asymptotic bound. The chain holds throughout the asymptotic regime; for small n with large a and small ℓ the bound is conservative, and tightens as $|a|^\ell$ decays.

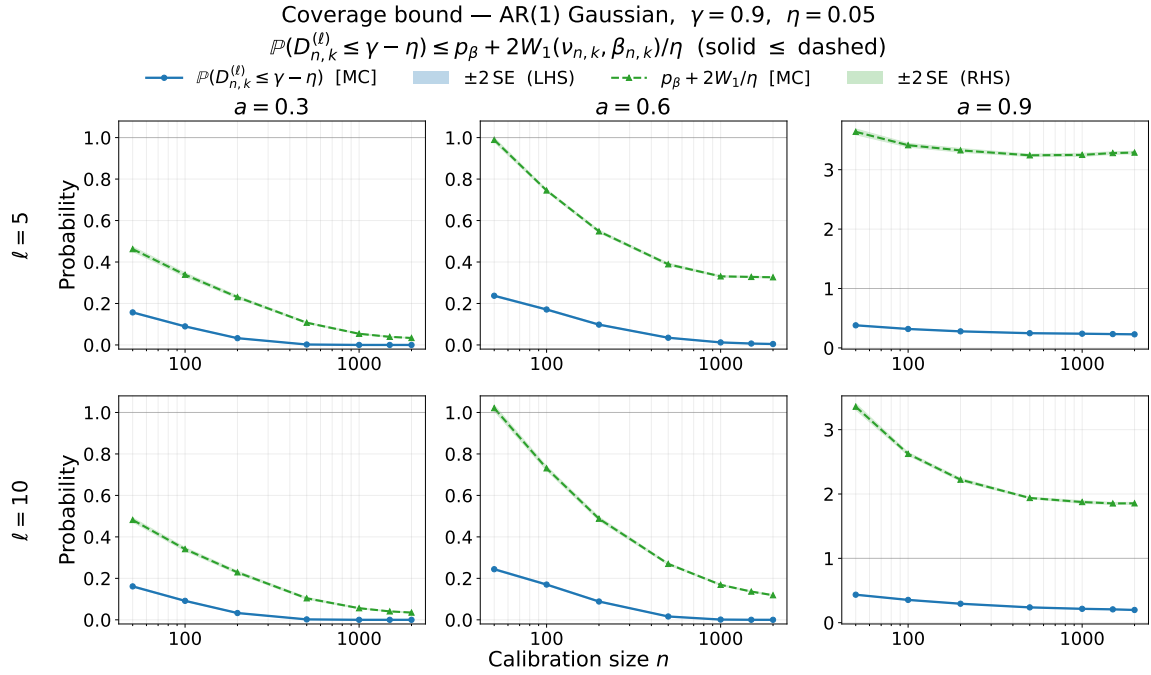


Figure 8: Bad-calibration bound from Theorem 12: $\mathbb{P}(D_{n,k_\gamma}^{(\ell)} \leq \gamma - \eta)$ (solid blue) against $\mathbb{P}(B_{n,k_\gamma} \leq \gamma - \eta/2) + 2W_1/\eta$ (dashed green) as a function of n , for $\gamma = 0.9$, $\eta = 0.05$, $a \in \{0.3, 0.6, 0.9\}$, and $\ell \in \{5, 10\}$. The bound can exceed one for large a and small ℓ , where the Markov penalty $2W_1/\eta$ dominates, and tightens as ℓ grows and W_1 decays.